Science Advances

AAAS

advances.sciencemag.org/cgi/content/full/4/4/eaan8917/DC1

Supplementary Materials for

Light-induced dynamic structural color by intracellular 3D photonic crystals in brown algae

Martin Lopez-Garcia, Nathan Masters, Heath E. O'Brien, Joseph Lennon, George Atkinson, Martin J. Cryan, Ruth Oulton, Heather M. Whitney

Published 11 April 2018, *Sci. Adv.* **4**, eaan8917 (2018)
DOI: 10.1126/sciadv.aan8917

The PDF file includes:

Other Supplementary Material for this manuscript includes the following:
(available at advances.sciencemag.org/cgi/content/full/4/4/eaan8917/DC1)

- movie S1 (.avi format). Three-dimensional autofluorescence confocal false-color maps showing the relative position between OPCs (red) and chloroplasts (green) within the epidermal cells.

- movie S2 (.avi format). Structural color decay for the two OPCs shown in Fig. 3C.
- movie S3 (.avi format). Structural color decay filmed with stereomicroscope under low magnification.
- movie S4 (.avi format). Fast decay of structural color for OPCs under continuous illumination.

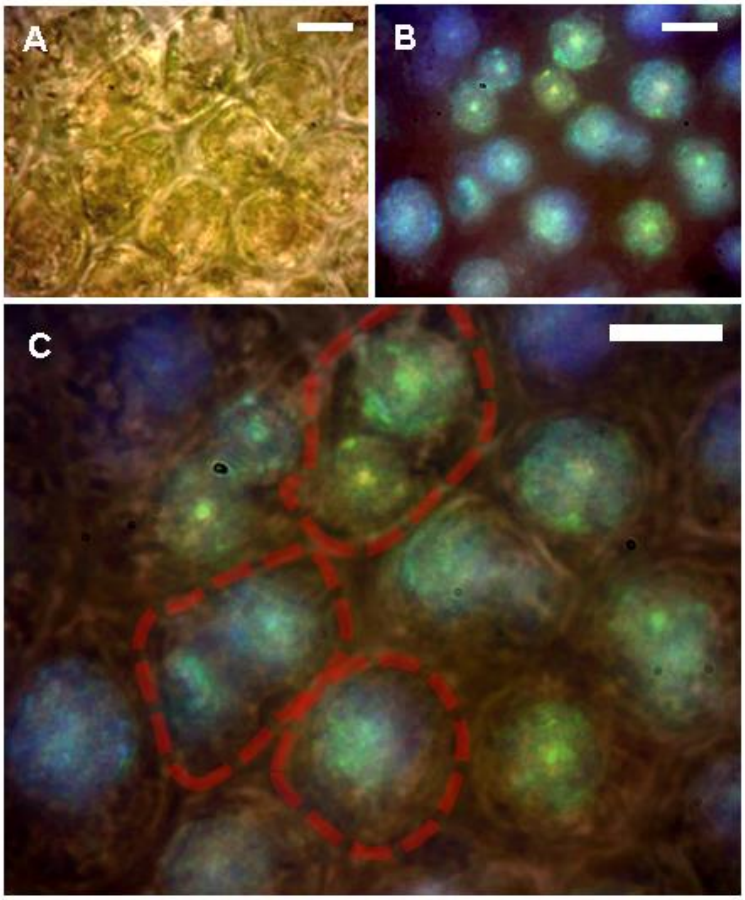

fig. S1. High-magnification in vivo optical microscopy (115×) images of the epidermal region. (**A**) transmission and (**B**) epi-illumination. In both cases focusing is at the OPCs within the epidermal cells. (**C**) Combination of (A) and (B) in the same image to highlight the position of the OPCs within the cell. Red dashed lines highlight the cell wall position for three different cells. Notice that one, two and sometimes three OPC vesicles have been seen within the same cell. Scale bar is 7 μm for all images.

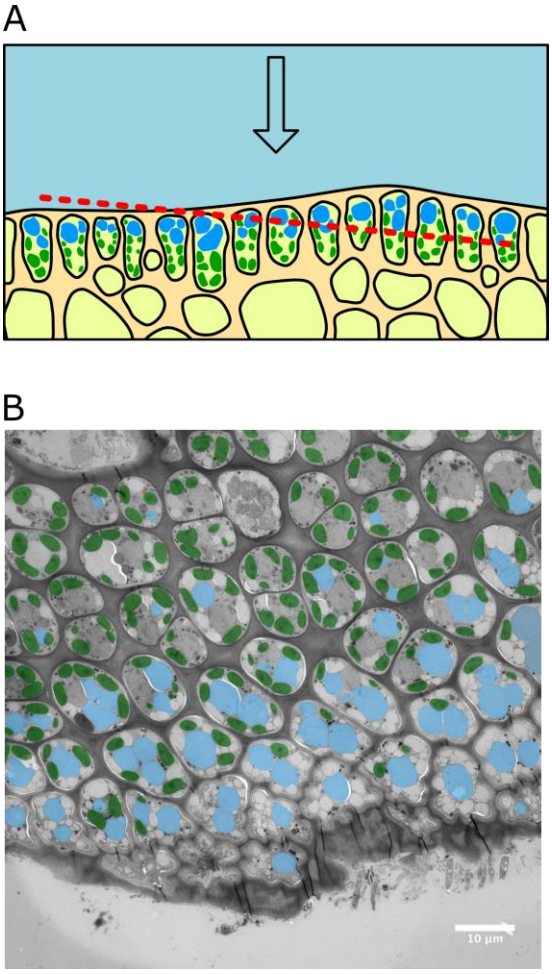

fig. S2. Position of the OPCs and chloroplast in the epidermal cells. (**A**) Sketch of epidermal cell morphology in *Cystoseira tamariscifolia. OPC* (blue), chloroplast (green) and epidermal cells are sketch in cross-section. The top black arrow indicates the incident light direction. Red dotted line shows the cut along the surface produced during the high pressure frozen TEM preparation process as shown in (B). (**B**) High pressure frozen TEM image of epidermal cells. Point of view is normal to the epidermis surface and the cut is tilted as illustrated in (A). The same configuration applies for images in Fig 2 of the main text. OPCs are shown in blue and chloroplast shown in green.

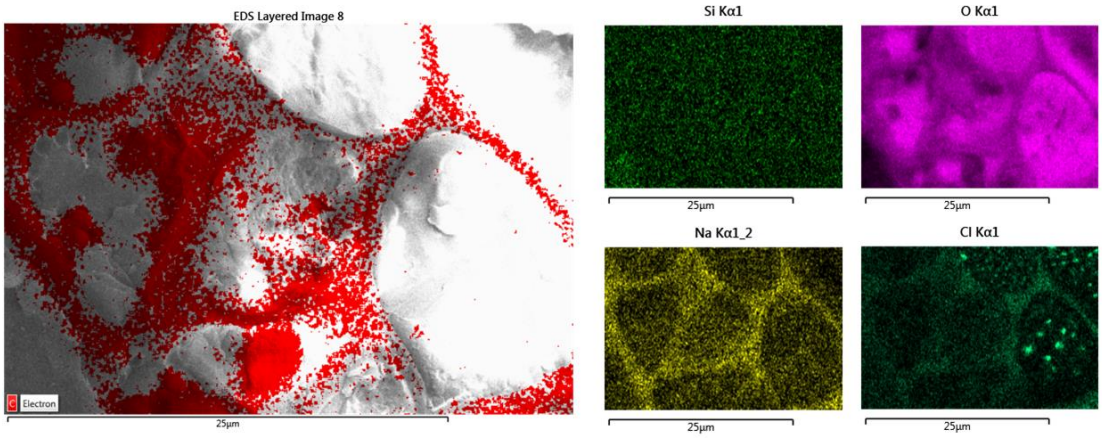

fig. S3. Energy-dispersive x-ray analysis over several epidermal cells containing OPCs. EDX analysis over several epidermal cells containing OPCs. Left image shows the measurement area. Red color shows carbon content. The right images show Si, O, Na and Cl concentrations. Pink shows Oxygen with high concentration within the cells. Silica (SiO_2) content is very low and uniformly distributed through the whole image. These results confirm our confocal fluorescent measurements (Fig 2) for the lipid based composition of the spheres.

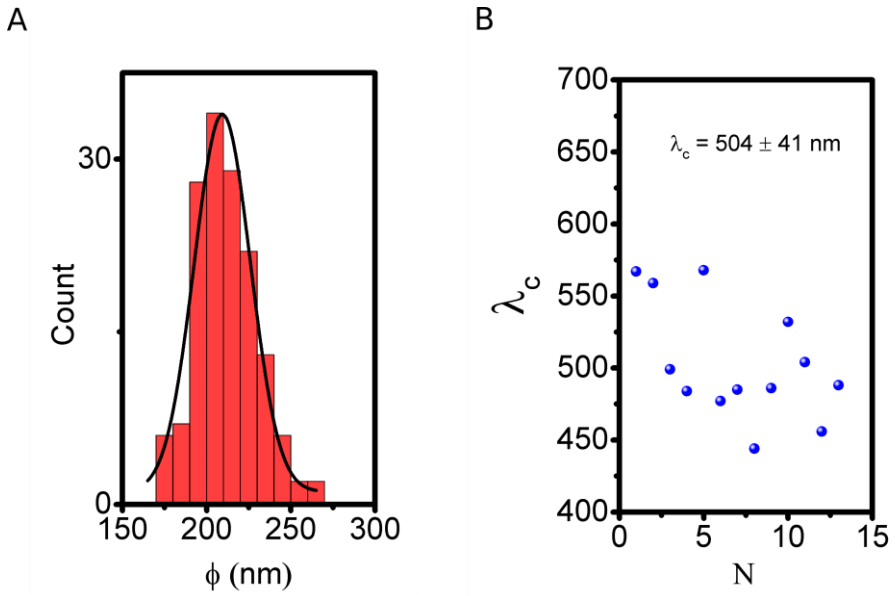

fig. S4. Statistical analysis of single OPC properties. (**A**) Diameter distribution for spheres within vesicles in different cells. Statistical analysis was performed on two different vesicles. Fitting shows that average diameter is $\phi_c = 209 \pm 1.3$ nm (Gaussian fit). The histogram shows that diameters in a range within $170 < \phi < 260$ nm can be found within the vesicles. Notice that the central value $\phi_c = 209 \pm 1.3$ nm corresponds to the two vesicles inspected for this example. It was not possible to relate the original iridescence color of the cell to the vesicles inspected by TEM, but this may be inferred by the slight differences in ϕ_c found for each vesicle. (**B**) Central wavelength of the reflectance peck at normal incidence for 15 different OPCs of the same specimen.

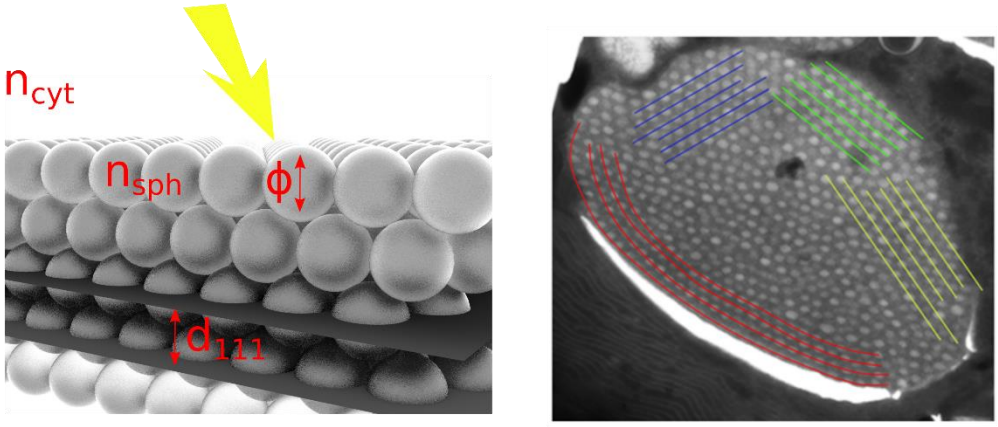

fig. S5. Arrangement of the spheres within the OPCs. (**A**) Schematic for the arrangement of the spheres in a close-packed FCC lattice showing the parameters to be considered in the model for calculation of the reflectance and Bragg diffraction approximation of a planar opal. n_{cyt} and n_{sph} are the refractive indices for surrounding media and nanospheres respectively. ϕ is the diameter of the spheres and d_{111} is the distance between planes of monolayer of spheres (see methods). $d = \sqrt{2}\phi$ is the lattice parameter (not shown) for an FCC lattice of close-packed spheres. (**B**) Different sets of planes highlighted in the same vesicle. Real values approximate to those obtained for d_{111} in the Bragg approximation used in the main text.

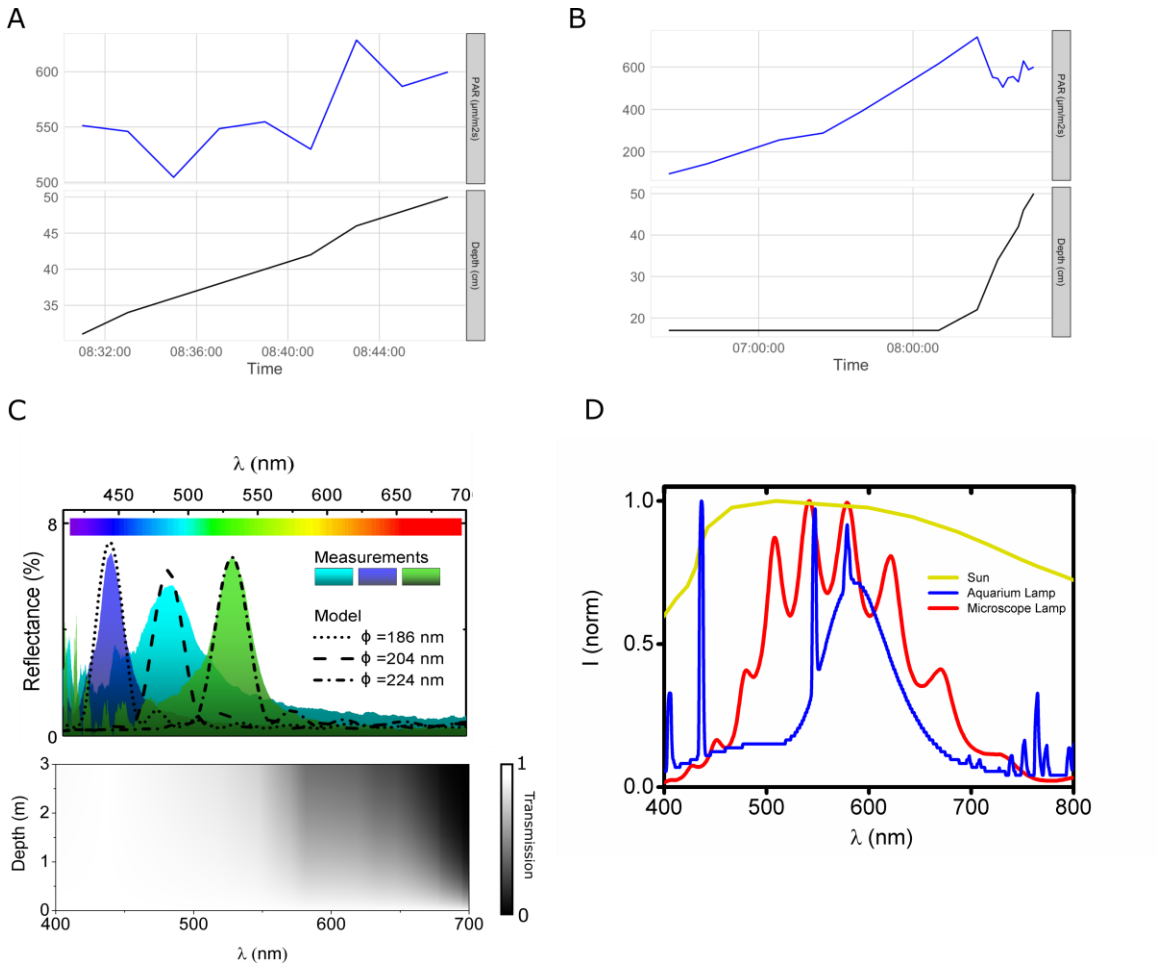

fig. S6. Relevant spectra and intensities for the light sources used in the experiments. (**A**) Photosynthetic Active Radiation (PAR) at rock pools measured in the South West coast of the UK and for the light. The measurement started 12th July 2016, 8:31am (3hrs after sunrise), low tide. Sky was clear. (**B**) Same location, measurement started 13th July 2016, 6:25 am (1hr after sunrise), low tide. Also clear sky. In both cases depths (water column over the algae) shows values relevant for the study performed in the aquarium. (**C**) Bottom: Calculated transmission of seawater as a function of wavelength and depths relevant for this study. The water column over the rock pool where the algae is found reaches ≈ 3m at high tide. Top: Experimental and calculate reflectance for several OPCs as shown in Fig 3A of the main text. Note higher irradiance will reach the algae for those spectral regions where the OPCs show a strong reflectance. Note that the PAR intensity will vary also due to weather conditions as for example clouds or turbidity of the water. We collected measurements under both cloudy and clear weather for comparison and found variations higher than several hundreds of µmol/m^2/sec between clouds and clear sky at midday. (**D**) Irradiance spectra for: lamp used in aquaria for dynamic iridescence study (blue), tungsten lamp used in the high magnification microscope (Thorlabs OSL-1) and solar spectra at sea level. The intensity was normalized to the maximum counts for easier comparison with the solar spectra at sea level.

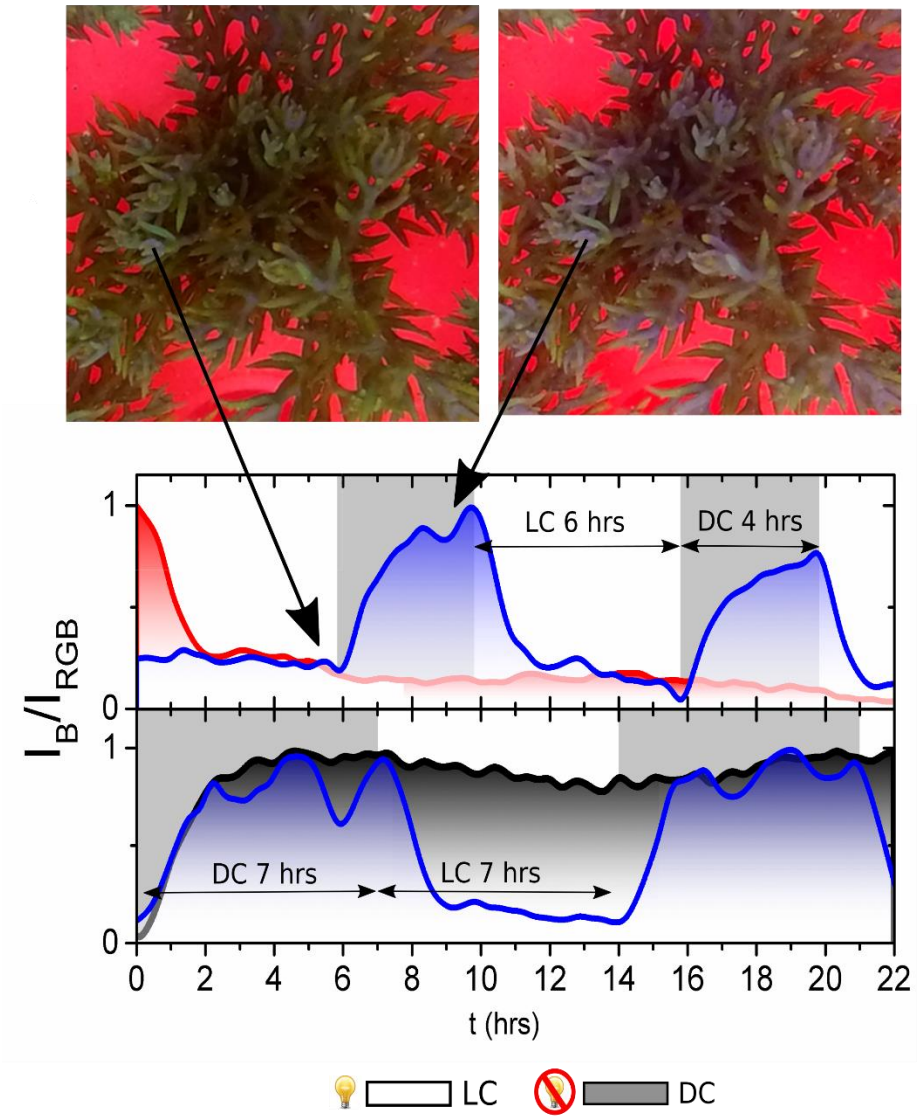

fig. S7. Dynamics of structural color. Structural color intensity is measured over images of the whole specimen (see examples at the top) as the ratio of total intensity in the blue channel to the total intensity in the three (RGB) channels of the CCD camera. Images were taken every 20 minutes for 24 hours while illumination is varied. Red and Black lines show the relative change in intensity captured by the blue channel of the camera (I_B/I_{RGB}) during continuous illumination and darkness respectively. In both cases period is 24 hours. Blue lines show two different patterns of illumination. **Top:** LC 6hrs / LD 4 hrs. **Bottom:** LC 7 hrs / DC 7 hrs. Note decay/recovery of iridescence always take place in ≈ 2-3 hrs independently of the illumination pattern. PAR intensity at the aquarium = 61.2 µmol/m^2s.

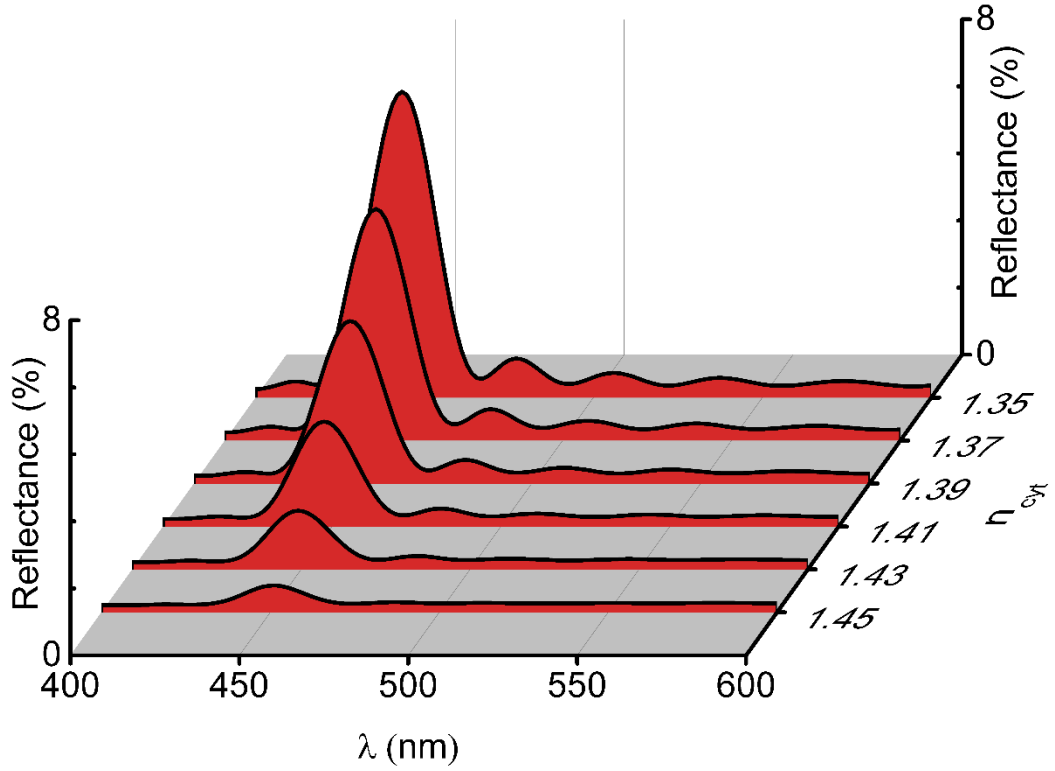

fig. S8. Calculated reflectance of an OPC as a function of cytoplasm refractive index. Calculated variation of the reflectance spectrum for an OPC with parameters shown in Fig. 3 and ϕ = 186 nm. n_{cyt} is varied between 1.35 and 1.45 whist the other parameters that define the optics of the OPC are kept constant.

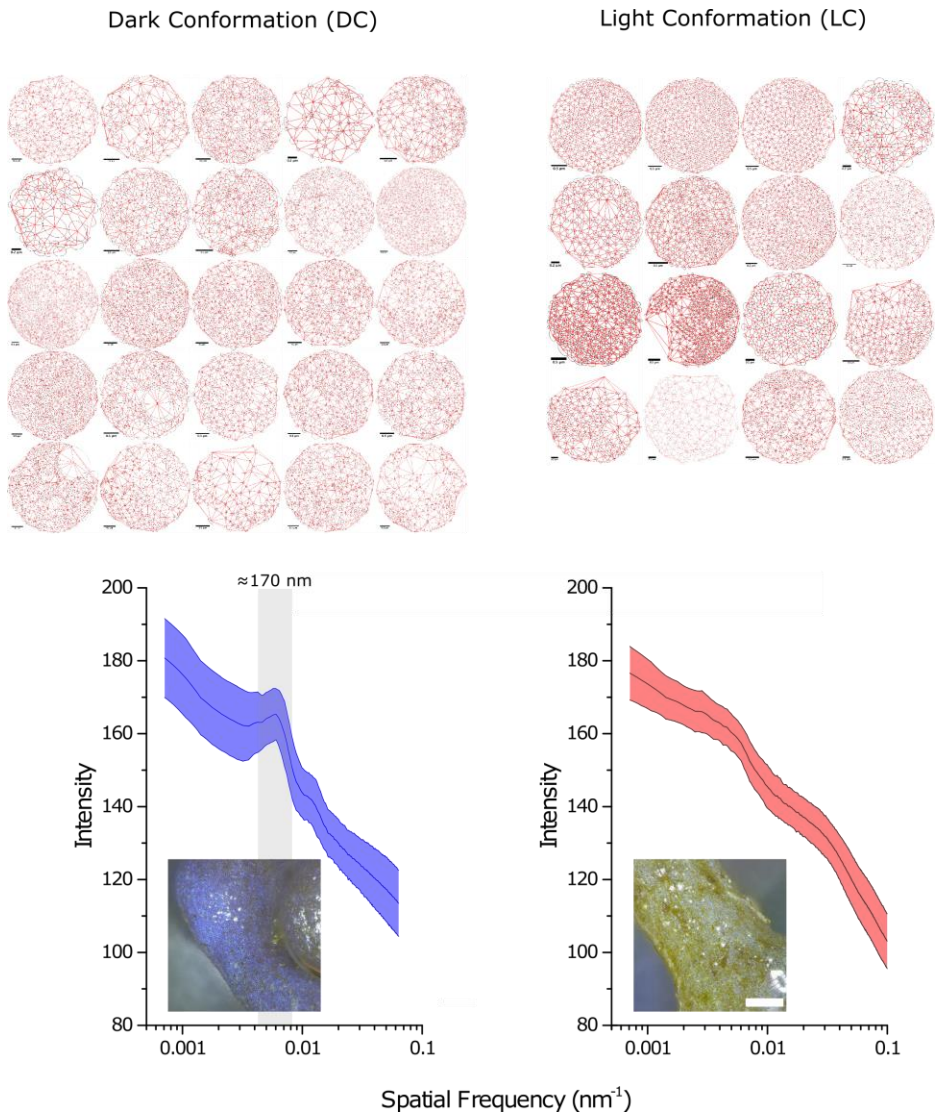

fig. S9. Statistical analysis of lattice expansion on OPCs between dark and light conformation. Top: Delaunay triangulation method applied to TEM images as shown in Fig 5A. 25 and 16 images for DC (blue, left) and LC (brown, right) light adapted OPCs respectively were used for the analysis. The resulting distances *d* were used to build the statistical analysis in Fig 5C of the main text **Bottom:** Fourier power analysis (29) over the same images and for the two light conformations. Thick shadow line indicates statistical data and thin inner line the average frequencies of all images. Spatial Frequencies for the peak on the blue line correspond to an approximate center-to-center lipid sphere distance of ≈170nm.

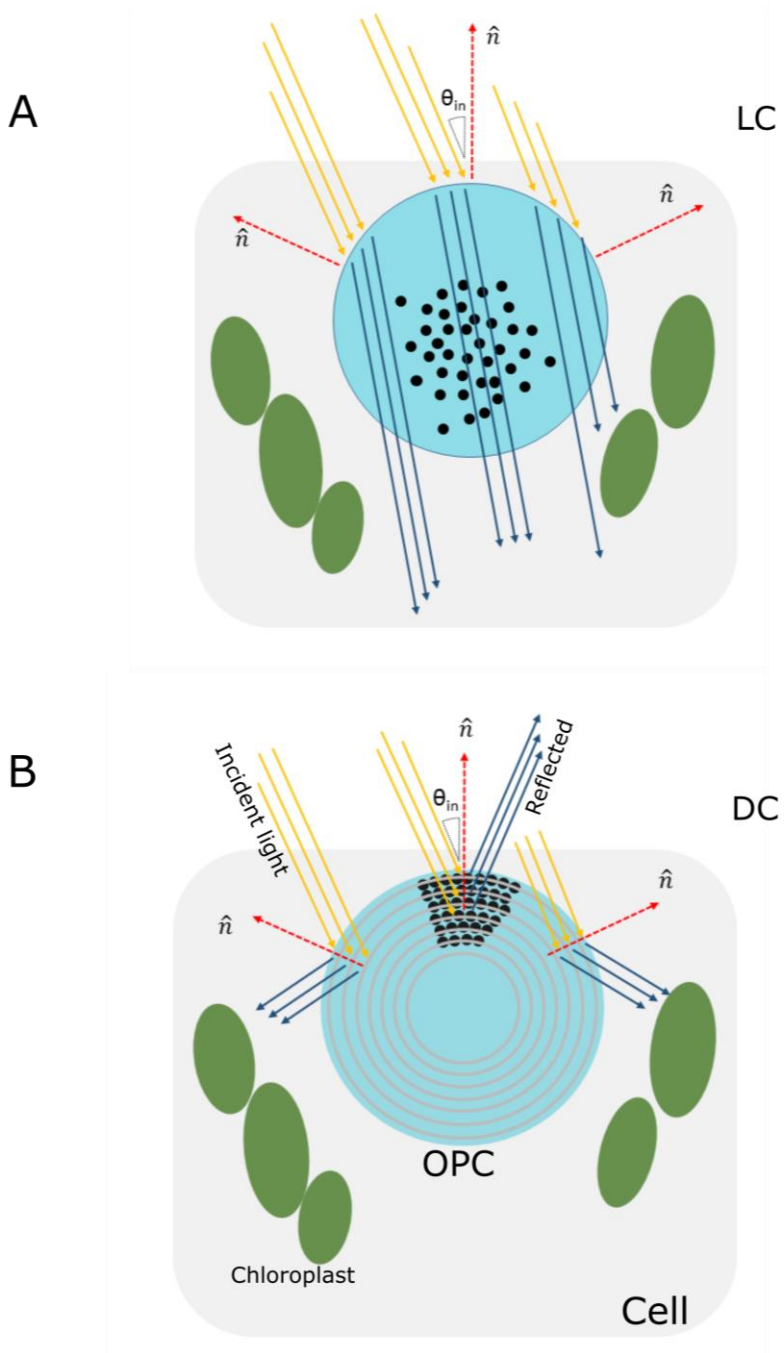

fig. S10. Sketches of possible mechanism for light flux redirectioning into the chloroplast. (**A**) OPC in Light Conformation (LC). Nanospheres are randomly distributed. (**B**) OPC in Dark Conformation (DC). The grey concentric lines are a guide to the eye for the different planes of close packed spheres distributed within the OPC. $\hat{\boldsymbol{n}}$ represents the normal to the surface of the OPC in each point, θ_{in} is the angle between the incidence beam and $\hat{\boldsymbol{n}}$ at each position. Yellow and blue lines represent incident and transmitted (A) or reflected (B) light respectively.

movie S1. Three-dimensional autofluorescence confocal false-color maps showing the relative position between OPCs (red) and chloroplasts (green) within the epidermal cells.

movie S2. Structural color decay for the two OPCs shown in Fig. 3C. They are located within the same cell and inspected under continual illumination by high magnification microscope. Video is shown at speed X20 faster than real time.

movie S3. Structural color decay filmed with stereomicroscope under low magnification. This video suggests the decay of single OPCs is triggered by adjacent ones already in a DC configuration. Therefore, the decay of iridescence of the whole specimen could be the final result of the combination of all the short-time iridescence decays of single OPCs when the uneven illumination over different areas of the whole specimen is considered. Note that the video has been speed up (x20 real time) to better highlight how the decay propagates through the epidermal cells.

movie S4. Fast decay of structural color for OPCs under continuous illumination. Strong redshift shown as a flash of green reflectance is observed for < 1 sec before the structural color decays completely. Video is X4 faster than real time for a better appreciation of the whole decay process.